Research Article Vol. 41, No. 6 / June 2024 / Journal of the Optical Society of America A B65

Journal of the Optical Society of America A

OPTICS, IMAGE SCIENCE, AND VISION

Long-term measurement and characterization of boundary layer optical turbulence

CHRISTOPHER JELLEN,[1,*] CHARLES NELSON,[2] CODY BROWNELL,[1] AND JOHN BURKHARDT[1]

[1]Mechanical Engineering Department, United States Naval Academy, 590 Holloway Rd Stop 11C, Annapolis, Maryland 21402, USA
[2]Electrical and Computer Engineering Department, United States Naval Academy, 597 McNair Rd, Annapolis, Maryland 21402, USA
*cdjellen@gmail.com

Received 7 February 2024; revised 9 April 2024; accepted 13 April 2024; posted 15 April 2024; published 3 May 2024

The United States Naval Academy long-term scintillation measurement campaign was a multi-year effort to characterize optical turbulence in the near-maritime atmospheric boundary layer (ABL). At its core, the field experiment consists of *in situ* measurements of bulk atmospheric and oceanographic parameters, as well as path-averaged measurements of the refractive index structure parameter, C_n^2, collected using a large-aperture scintillometer. The field experiment ran from January 1st, 2020, through September 26th, 2023, representing the most comprehensive collection of optical turbulence measurements in the near-maritime ABL to date. Long-term measurements enable researchers to evaluate existing theory and develop new models applicable to this environment. The present study characterizes some of the physical relationships that affect optical turbulence. This characterization focuses on the relationship between local optical turbulence and select atmospheric and oceanographic parameters. The impact of temperature gradients on the extent of optical turbulence was analyzed, along with its interactions with relative humidity and wind speed. The diurnal and seasonal variations in measured C_n^2 were examined, with comparisons drawn against other environments. Further information and the full dataset are publicly available through the optical turbulence benchmark repository [Jellen *et al*., GitHub, 2023].

https://doi.org/10.1364/JOSAA.520980

1. INTRODUCTION

The United States Naval Academy (USNA) long-term scintillation measurement campaign was a multi-year effort to characterize the atmospheric boundary layer (ABL) above the Severn River at USNA in Annapolis, Maryland. The Severn River is a tidal estuary that flows into Chesapeake Bay near USNA. This propagation environment has been characterized as near-maritime [1,2]. Turbulence in the ABL is the result of temperature gradients above the water, winds that pass over land masses to the north-east and south-west of the propagation path, and many other factors [2–7]. The aim of this field experiment was to measure a set of the bulk atmospheric and oceanographic parameters that could contribute to turbulence in the ABL, as measured through optical turbulence. The measurements were collated into a new, publicly available dataset, available in two formats through the optical turbulence benchmark repository.

At its core, this dataset consists of *in situ* measurements of bulk atmospheric and oceanographic parameters and path-averaged measurements of the refractive index structure parameter, C_n^2. Measurements of C_n^2 were collected using a ScinTec BLS 450 large-aperture scintillometer [8]. The 890 m propagation path between the scintillometer receiver and transmitter crosses the Severn River at a height of approximately 3 m. The field experiment was conducted between January 1st, 2020, and September 26th, 2023, chiefly as a tool for macrometeorological theory and model evaluation, and to develop new models of optical turbulence. Bulk atmospheric and oceanographic measurements were collected at two co-located weather and coastal observation stations, and at one sea-surface temperature buoy in Chesapeake Bay.

Characterizing optical turbulence in the ABL is an ongoing challenge, with active research into the underlying physics that drive variations in the refractive index [4,9]. Both physics-based and data-driven bulk-atmospheric models for predicting optical turbulence have been applied in the near-maritime ABL [4,10,11]. The data generated during the field experiment are essential in evaluating the applicability of these and future models. Monin–Obuhkov similarity theory (MOST) and MOST-based models for near-maritime optical turbulence are an active area of research [4,6].

The primary aim of this study is to describe and release the field experiment dataset, enabling research teams to further investigate and characterize optical turbulence in the near-maritime ABL. The significant temporal coverage may enable these teams to understand this environment with higher confidence. A secondary aim of the study is to identify the similarities and differences between optical turbulence in the near-maritime ABL and other propagation environments. This component of the analysis investigates the strength of diurnal patterns in

measured optical turbulence, seasonal variation in turbulent intensity, and the impact of temperature differences between the atmosphere in the ABL and the water surface below. The impacts of temperature gradients, relative humidity, and bulk wind speed on optical turbulence in the ABL are assessed using the full dataset. The strength of diurnal and seasonal trends in measured C_n^2 are also investigated and contextualized against other propagation environments.

2. FIELD EXPERIMENT

Characterizing turbulence in the ABL presents an operational challenge due to the range of atmospheric and oceanographic phenomena that contribute to observed optical turbulence along a path. These phenomena are dynamic, and measurements often change quickly in time [3]. Their dynamic range may be determined in part by seasonal variation [2]. The USNA long-term scintillation measurement campaign sought to address these challenges by collecting data over a period of 45 months, obtaining bulk atmospheric measurements in the vicinity of the scintillometer receiver, and by leveraging multiple observation stations in data collection.

Measuring variations in the refractive index in the ABL requires specialized equipment and a reasonable collection frequency. The measurement frequency was balanced against the quality of measurements, which are estimated from higher-frequency samples. To obtain a measure of path-averaged C_n^2 across the Severn River, a ScinTec BLS 450 large-aperture scintillometer link was established between between the USNA Santee Basin on the Western shore and the Waterfront Readiness Center on the Eastern shore. The path between the scintillometer's transmitter and receiver is pictured in greater detail in Fig. 1.

In Fig. 1, the scintillometer transmitter (labeled 1) provided a 5 Hz pulsed source of 880 nm wave fronts, which traveled approximately 890 m across the Severn River to the receiver (labeled 4). The scintillometer determined a measure of C_n^2 from the degraded wave fronts at the receiver, reporting every minute. Bulk atmospheric and oceanographic measurements were collected near the scintillometer receiver. The National Oceanic and Atmospheric Administration (NOAA) Coastal Observation station 8575512 is labeled 2 in Fig. 1 [12]. This station collected atmospheric measurements at heights of between 5 m and 10 m above the water, as well as the water's surface temperature at a 6 min frequency. An additional Davis Vantage PRO2 weather station (labeled 3) was established to provide further coverage of standard atmospheric measurements, as well as other features including solar radiation incident at the surface [13]. Oceanographic data from these stations were augmented using hourly measurements of sea-surface temperature from the National Data Buoy Center (NDBC). Thomas Point station TPLM2 is approximately 12 km Southwest of USNA [14].

Measurements from these sources were collated into a single, annotated netCDF4 file. The netCDF format allows datasets to specify static attributes such as station location, as well as measurement details such as units alongside the measured values [15]. The characteristics of each station and its measurements are highlighted in greater detail in Table 1.

Data were available for all of the sources in Table 1 for the duration of the study, with the exception of short-term and long-term outages in some measurement instruments. The availability and characteristics of the measurements collected are explored in greater detail in Section 3.

3. DATA

Each data source used to characterize the local propagation environment for the duration of the study generated reports in different formats and frequencies. While each set of measurements itself presents a window into the ABL, the composition of these measurements provides a better tool for modeling and characterization. To simplify the process of identifying trends or correlations between features, the data were re-indexed using the scintillometer's onboard clock frequency. A measurement of C_n^2, or an indicator for a missing value, is available for each minute (inclusive) between January 1st, 2020, and 10:45 EST on September 26th, 2023. Bulk atmospheric and oceanographic

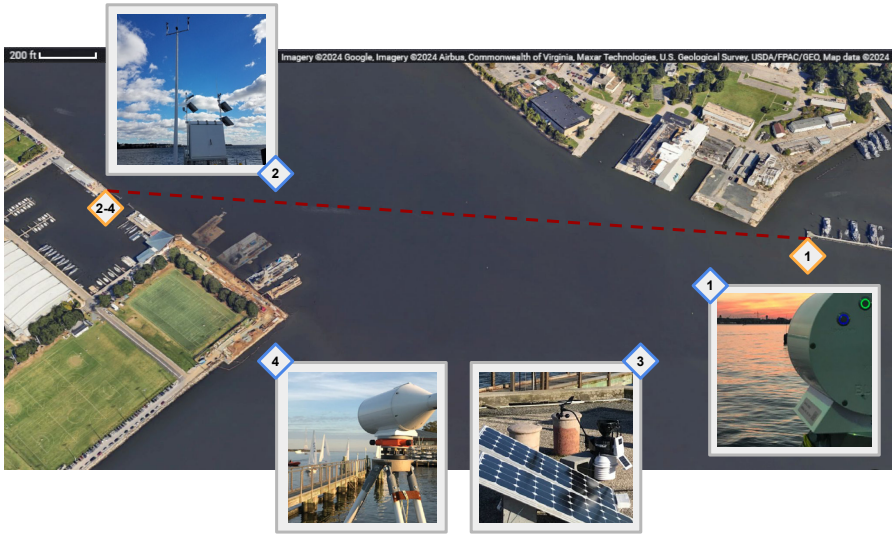

Fig. 1. Overview of the United States Naval Academy Boundary Layer Scintillometer Link.

Table 1. Data Sources Used in the United States Naval Academy Long-Term Scintillation Measurement Campaign

	Parameter	Short Name	Description	Units	Heights [m]
Station 8575512	Wind direction	Dir.10m	Mean wind direction	°	10
	Wind speed	Spd.10m	Mean wind speed	ms^{-1}	10
	Air pressure	P.10m	Barometric pressure	mbar	10
	Air temperature	T.5m	Ambient air temperature	°C	5
	Water temperature	T.0m	Water surface temperature	°C	0
Vantage PRO2	Wind direction	Dir.3m	Mean wind direction	ms^{-1}	3
	Wind speed	Spd.3m	Mean wind speed	ms^{-1}	3
	Air pressure	P.3m	Barometric pressure	mbar	3
	Air temperature	T.3m	Ambient air temperature	°C	3
	Relative humidity	RH.3m	Ambient relative humidity	%	3
	Solar radiation	Rad.1m	Incoming total solar radiation at ground level	W^2m^{-1}	1
TPLM2	Water temperature	T.0m.2	Water surface temperature	°C	0
BLS 450	Refractive index structure parameter C_n^2	Cn2.3m	Optical turbulence strength	$m^{-\frac{2}{3}}$	3

measurements were re-indexed using the time index provided by the scintillometer. These re-indexed measurements were not interpolated so that an instrument reporting a value every 10 min will have values only every 10 min in the final dataset.

A. Measurement Availability

The data sources described in Section 2 include quality-control features that remove malformed sensor data [12–14]. Records that did not pass quality control or were unavailable due to sensor failure appear in the dataset as missing measurements. While data were generally available from all sources for the duration of the study, there were major and minor interruptions in some of the parameters in Table 1. The most significant of these interruptions were for Station 8575512 and for NDBC's TPLM2. The first was under maintenance at the start of the study, coming online in mid June of 2020. In the case of TPLM2, the water temperature sensors were removed in mid July of 2022 and were unavailable for the remainder of the study. Misalignment during the month of July 2023 led to a significant number of missing measurements by the scintillometer. All instrument degradations were characterized in terms of their measurement availability, the proportion of possible measurements that are present in the dataset during a given month (Fig. 2).

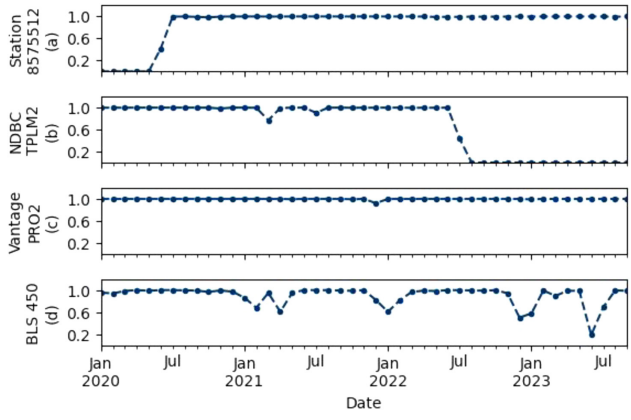

Fig. 2. Proportion of measurements passing quality control for each data source during duration of the field experiment.

The parameters in Table 1 are grouped by instrument, and they generally had outages on the order of days, with the exception of the two major degradations (described in Section 3.1) and the scintillometer (described in the last row of Fig. 2). One period of significant measurement availability degradation occurred during July 2023 due to instrument misalignment. Inclement weather, misalignment, and power outages resulted in three periods of moderate availability degradation in the early spring of 2021, early 2022, and the winter of 2022. Given the duration of the measurement campaign, measurements of C_n^2 were collected during all seasonal conditions.

B. Descriptive Statistics

For each numerical parameter in the USNA long-term scintillation dataset, the number of available measurements, mean value, and standard deviation are reported in Table 2.

The descriptive statistics in Table 2 highlight the finding that C_n^2 is generally higher and more variable in the near-maritime ABL than in other high-altitude or over-land propagation environments [2–4,6,7,16]. The alignment between the measured air temperatures at Station 8575512 and the Vantage PRO2 are promising given the close proximity of the collection instruments. The differences in the measured mean and standard deviation in the wind speed could be partially attributed to the difference in elevation between the wind speed monitors of these two instruments. Measured water temperature was generally lower at NDBC TPLM2; this could be due in part to a difference in the depth of the water at which the station obtains measurements [14].

4. ANALYSIS

The dataset generated from the USNA long-term scintillation measurement campaign provides a rich source for characterizing and contextualizing optical turbulence in the near-maritime boundary layer. Greater availability of data also aides in characterizing the dynamics that impact the intensity of optical turbulence. This study focuses primarily on presenting the dataset as a tool for future analysis. To demonstrate the value

Table 2. Data Sources Used in the United States Naval Academy Long-Term Scintillation Measurement Campaign

	Parameter	Short Name	Mean Value	St. Dev.	Count	Units
Station 8575512	Wind direction	Dir.10m	198.3	97	285,609	°
	Wind speed	Spd.10m	2.8	1.9	285,609	ms^{-1}
	Air pressure	P.10m	1016.8	7.3	319,660	mbar
	Air temperature	T.5m	15.2	9.2	326,854	°C
	Water temperature	T.0m	18.1	8.9	284,830	°C
Vantage PRO2	Wind speed	Spd.3m	1.2	0.97	185191	ms^{-1}
	Air pressure	P.3m	1017.7	7.6	185,189	mbar
	Air temperature	T.3m	15.9	9.7	183,279	°C
	Relative humidity	RH.3m	74.3	16.3	183,313	%
	Solar radiation	Rad.1m	168.5	259	183,393	W^2m^{-1}
TPLM2	Water temperature	T.0m.2	15.0	8.9	21,940	°C
BLS 450	Refractive index structure parameter C_n^2	Cn2.3m	1.83×10^{-14}	3.49×10^{-14}	1,775,479	$m^{-\frac{2}{3}}$

of the dataset, the impact of the bulk temperature gradient in the near-maritime ABL on optical turbulence was analyzed and compared with prior studies. This analysis was followed by a deeper investigation into the interaction between relative humidity, local wind speed, and temperature gradients. The final application of the dataset described in this study is in identifying diurnal and seasonal patterns in measured C_n^2. All these characterizations were explored in detail using the 45 months of available field data.

A. Temperature Gradients

Prior studies have identified the temperature gradient between the air along the propagation path and the water surface below as a key driver of turbulent effects in the near-maritime ABL [2,4,6]. These studies suggest that when the magnitude of this temperature gradient is large, measured C_n^2 may be higher. The temperature gradient in the near-maritime ABL results from temperature differences between the air and water [4]. The relationship between the air–water temperature difference and the extent of measured C_n^2 is described visually in Fig. 3.

In Fig. 3, the air–water temperature difference is computed using data obtained by Station 8575512 (T.5m and T.0m for air and water temperature, respectively, in Table 1). These temperature measurements were available between June 17th, 2020, and September 26th, 2023, with few interruptions, as seen in Fig. 2. The relationship in Fig. 3 between measured C_n^2 and the air–water temperature difference above the Severn River indicates that turbulent effects are lowest when the temperature difference is near 0°C. As the magnitude of the temperature difference increases, the extent of optical turbulence along the path tends to increase. The general climatological characteristics of the Severn River watershed result in a negative air–water temperature difference for much of the year, reflected by the high density between 0°C and −10°C in Fig. 3. These results reinforce the trends identified in [2,4,6]. Notably, the extent of measured optical turbulence generally scaled with the magnitude of the temperature difference between the air and water below the beam. This may help explain the absence of a strong diurnal pattern in measured C_n^2 identified in [4].

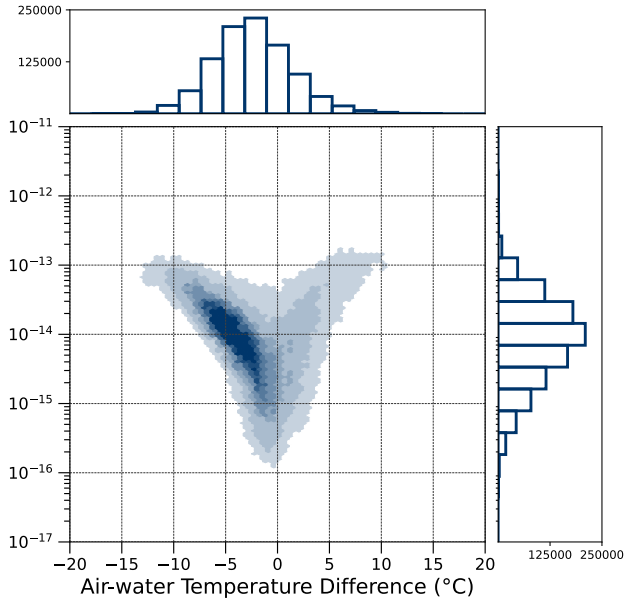

Fig. 3. Joint distribution of air–water temperature difference and measured C_n^2.

1. Interaction with Relative Humidity

The temperature gradient alone does not fully determine the extent of optical turbulence, either under MOST or from prior field experiments [2–4]. The potential impacts of other bulk-atmospheric parameters on C_n^2, including wind speed and relative humidity, were studied to better understand these effects. Interactions between the measured relative humidity and the temperature gradient's impact on C_n^2 are presented in Fig. 4.

In the near-maritime ABL above the Severn River, relative humidity tends to be high throughout the year. The top quintile of measured values for the duration of the study were at or above 90%, while the bottom quintile were at or below 60%. As shown in Fig. 4(a), there was no apparent, direct correlation between the measured relative humidity and C_n^2. The interaction between relative humidity and the temperature gradient studied in Section 4.A is notable in that the range of air–water temperature differences was narrow when humidity was high.

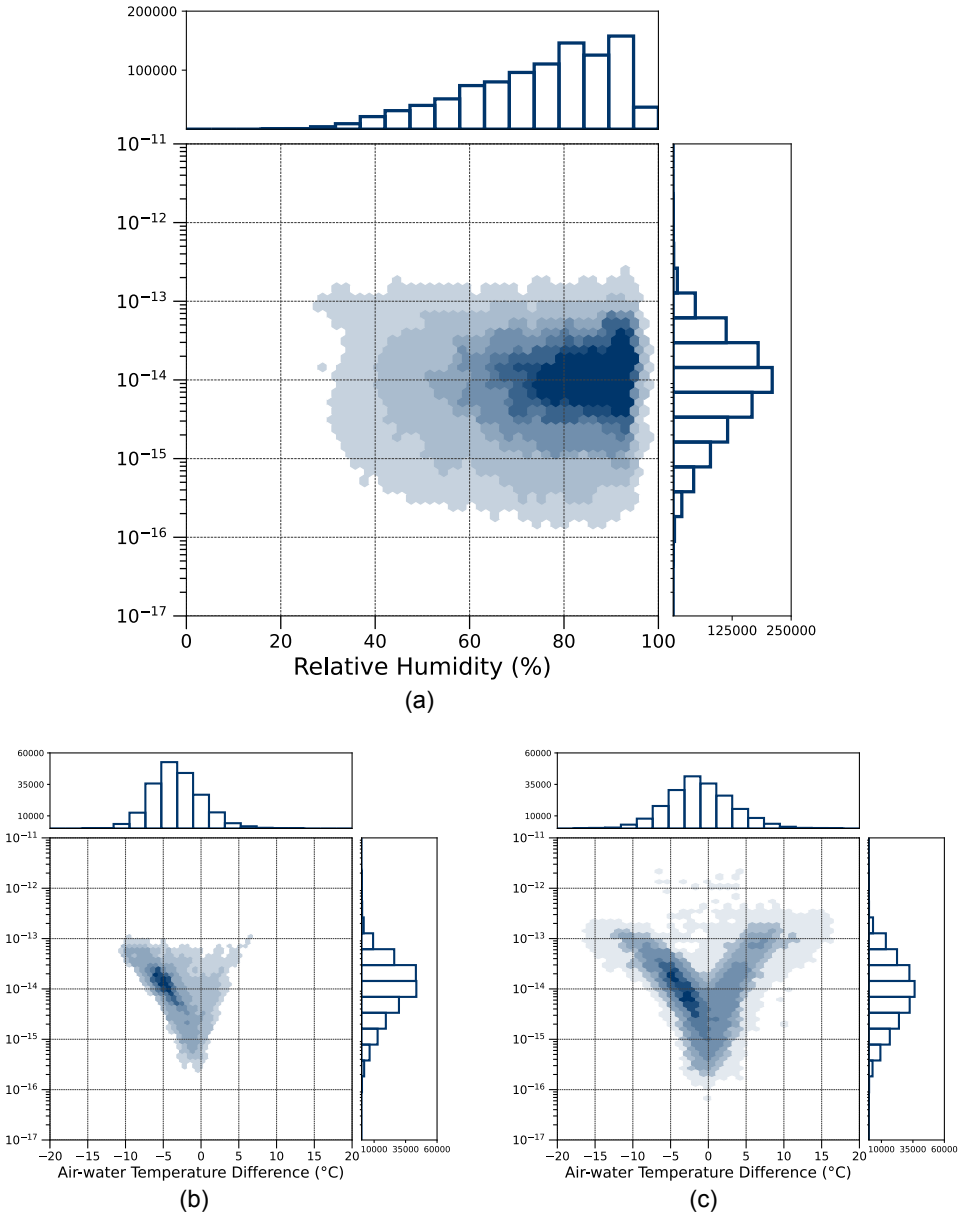

Fig. 4. Interaction between relative humidity, C_n^2, and the temperature gradient. (a) Joint distribution of relative humidity and C_n^2, (b) high relative humidity ($\geq 90\%$), (c) low relative humidity ($\leq 60\%$).

The distribution of measured C_n^2 during times of high humidity [Fig. 4(c)] was narrower and with a slightly higher mean value than in low-humidity cases [Fig. 4(b)].

2. *Interaction with Local Wind Speed*

The measured wind speed may reflect turbulent mixing dynamics in the near-maritime ABL [2–4,7]. This may directly impact the extent of optical turbulence, as well as the effects of the temperature gradient on optical turbulence. The top quintile of measured wind speed, collected at 10 m, was at or above 4.0 ms^{-1}, while the bottom quintile was at or below 1.2 ms^{-1}. These relationships are explored in Fig. 5.

While no strong trend was identified between measured wind speed and C_n^2 in Fig. 5(a), low-turbulence measurements at or below 1×10^{-15} were rarely observed when wind speed was above 6 ms^{-1}. Turbulent mixing enhanced by local wind effects may establish a floor for C_n^2 when bulk wind speeds are at or above this 6 ms^{-1} threshold. The differences between the distributions in Figs. 5(b) and 5(c) also reflect this trend, with higher C_n^2 during high wind speed events.

B. Diurnal Variation in Measured C_n^2

Measurement campaigns in over-land propagation environments have identified a strong diurnal trend in measured C_n^2 [16]. This relationship may result from the temperature gradient induced by time-dependent solar radiation incident on the ground [16]. Prior studies examined the strength of diurnal variations, suggesting the possibility of seasonal patterns in the

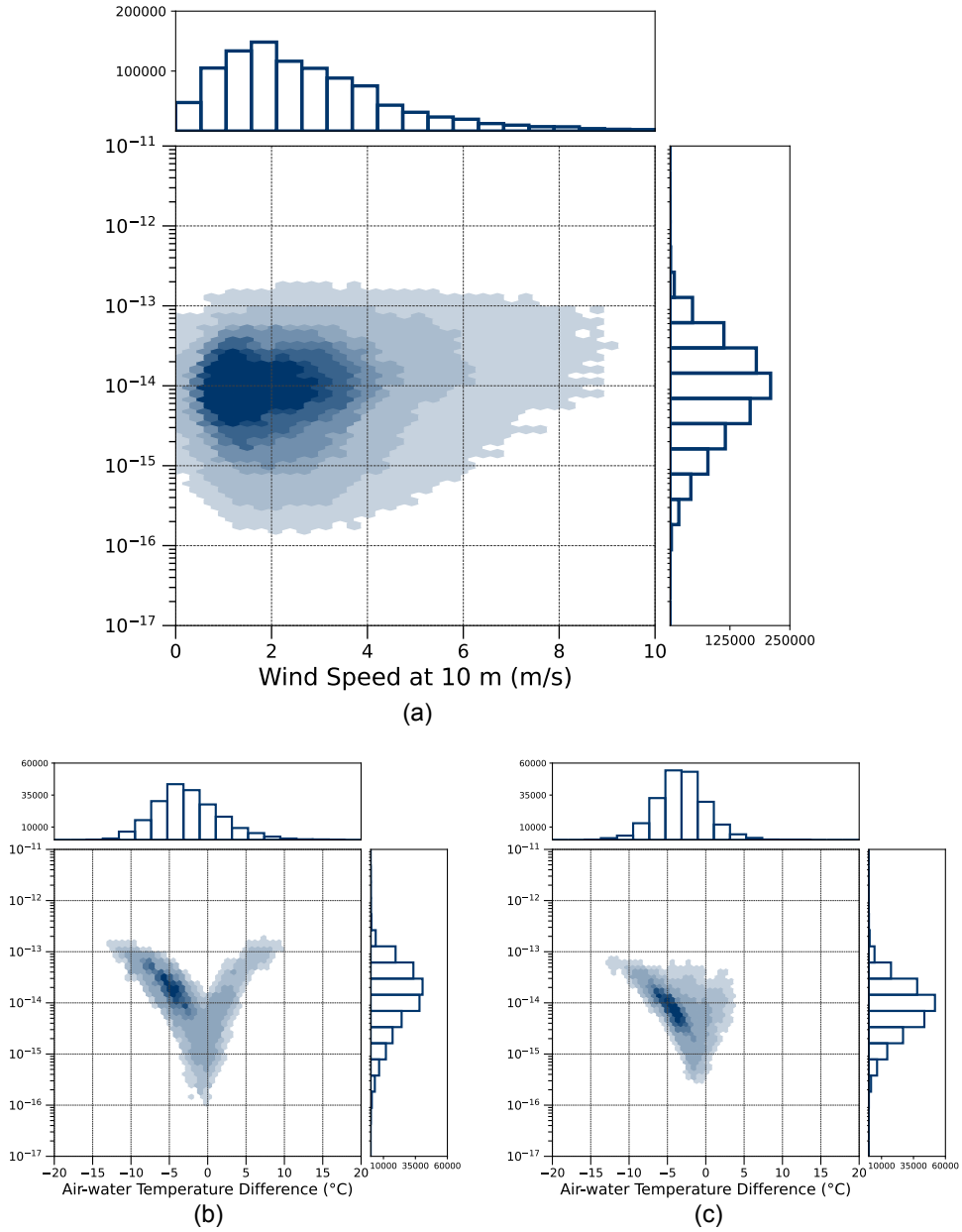

Fig. 5. Interaction between wind speed, C_n^2, and the temperature gradient. (a) Joint distribution of wind speed and C_n^2, (b) high wind speed ($\geq 4.0m$), (c) low wind speed ($\leq 1.2m$).

near-maritime ABL [2,7]. A similar study in the near-maritime ABL found that optical turbulence in the near-maritime ABL "generally does not show the strong diurnal variations that are observed over land" [4]. To investigate the strength of diurnal patterns, the distribution of measured C_n^2 at daytime (between local sunrise and local sunset) was compared to the distribution for nighttime (between local sunset and next-day's local sunrise) in Fig. 6.

The strong diurnal pattern observed in over-land links, such as in [16], is not readily apparent in the near-maritime ABL. The strength of optical turbulence tended to be slightly higher during the daytime, as seen in Fig. 6(a). The diurnal trend is also difficult to identify in Fig. 6(b), relative to the trend expected for an over-land link in [16]. The extent of measured C_n^2 did not appear to demonstrate obvious periodicity with the time since local sunrise. These results conform to the expectations of prior field experiments in similar environments [4].

C. Seasonal Variation in Measured C_n^2

The bulk atmospheric, oceanographic, and optical turbulence measurements from Tables 1 and 2 provide a source for statistical analysis and modeling of optical turbulence in the near-maritime ABL. One key question, difficult to address without long-term measurement, is that of seasonal trends in the distribution of observed C_n^2. The relationship between the air–water temperature difference and C_n^2 over the course of the year is described in greater quantitative detail in Table 3.

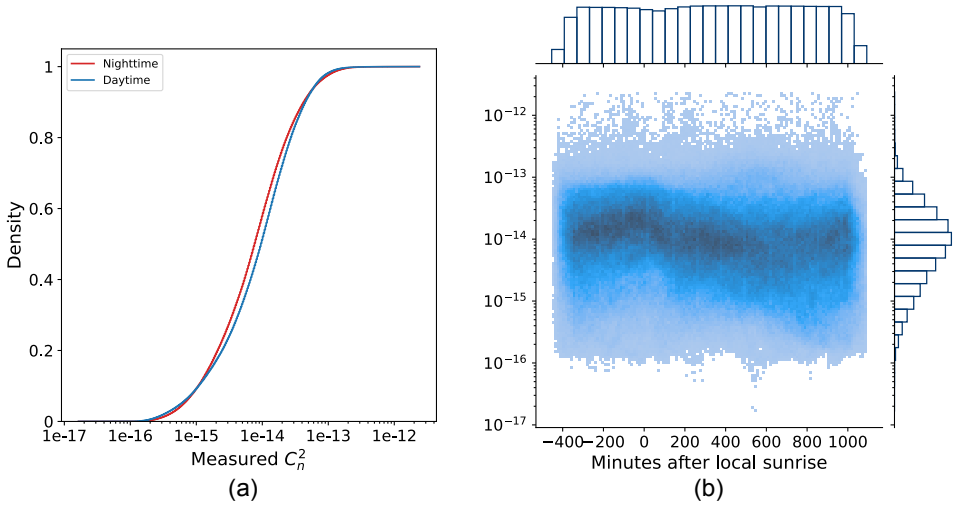

Fig. 6. Distribution of measured C_n^2 relative to local sunrise. (a) Cumulative distribution of C_n^2 in daytime (red) and nighttime (blue), and (b) joint distribution of C_n^2 and time elapsed since local sunrise.

Table 3. Monthly Mean Measurements of C_n^2 and Air–Water Temperature Difference (`T.5m− T.0m`)

	Jan	Feb	Mar	Apr	May	Jun	Jul	Aug	Sep	Oct	Nov	Dec
C_n^2 ($m^{-\frac{2}{3}}$)	2.10×10^{-14}	2.77×10^{-14}	2.62×10^{-14}	1.89×10^{-14}	1.48×10^{-14}	9.65×10^{-15}	1.01×10^{-14}	1.24×10^{-14}	1.72×10^{-14}	1.79×10^{-14}	2.54×10^{-14}	2.22×10^{-14}
AWT (°C)	−2.2	−1.0	−0.5	−0.9	−1.7	−1.7	−2.2	−3.1	−3.9	−3.8	−3.6	−2.9
Daytime	−1.5	−0.1	0.5	0.3	−0.7	−0.7	−1.1	−2.0	−2.7	−2.7	−2.4	−2.1
Nighttime	−2.8	−1.6	−1.5	−2.3	−3.0	−3.2	−3.8	−4.4	−5.12	−4.8	−4.5	−3.4

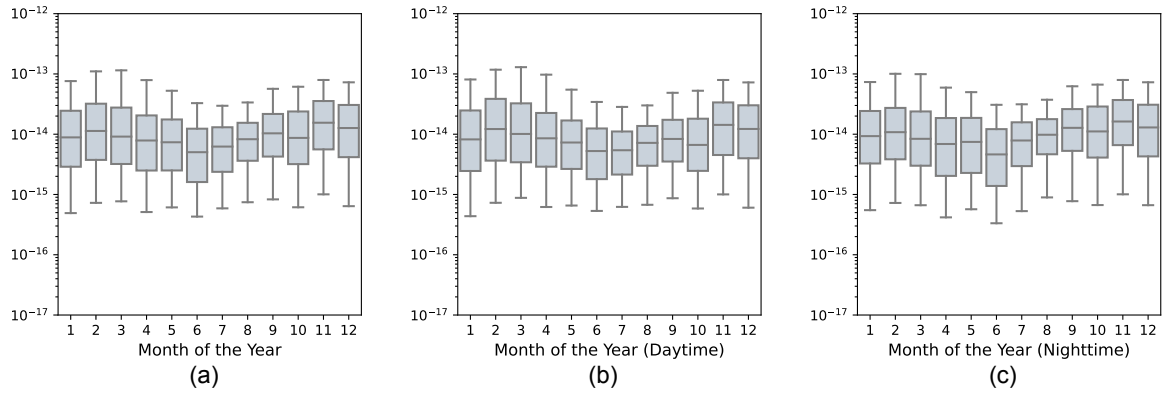

Fig. 7. Measured C_n^2 by month and separated into daytime and nighttime monthly aggregates, 5th to 95th percentiles.

In Table 3, the measured air–water temperature difference appeared lowest in magnitude between February and June, especially during the daytime, while this does not appear to reflect lower aggregate values of C_n^2 during the full period. Although temperature gradient effects appear to strongly influence optical turbulence in the near-maritime ABL, the direct seasonal variation in C_n^2 appears weak. The dynamic range of C_n^2 for each month, in aggregate and separated by day or night, is presented in Fig. 7.

The strength of optical turbulence in Fig. 7 tended to be highest in February, March, November, and December. Observed values were similarly lower and with smaller variance in June, July, and August. The time of year does not appear to meaningfully determine the strength of optical turbulence in the near-maritime ABL in Fig. 7. This relationship may warrant further study in over-land and open-ocean environments, as well as decomposition of seasonal effects on the drivers of turbulence in the ABL.

5. CONCLUSION

The USNA long-term scintillation measurement campaign collected bulk atmospheric, oceanographic, and path-averaged C_n^2 in the near-maritime ABL over a period of 45 months. The resulting dataset adds a rich source of real-world data, enabling research teams to develop and validate their understanding of

optical turbulence in the near-maritime ABL. Analysis of this dataset identified generally stronger optical turbulence in the near-maritime ABL when compared to over-land propagation environments. The relationship between the air–water temperature difference and C_n^2 in the ABL was characterized and contextualized using prior studies. While local humidity and bulk wind effects did not directly determine C_n^2, each affected the temperature gradient's impact on optical turbulent effects. Additionally, the absence of strong diurnal patterns and seasonal trends was identified from the field measurements. These insights are the first of many potential improvements in the understanding and modeling of turbulent effects in the near-maritime ABL.

Future investigations using this dataset on the applicability of current physics-based, MOST, macro-meteorological, and machine learning models may offer further insights. The dataset also has applications in deeper analysis of bulk atmospheric affects and interactions on measured optical turbulence. By making the dataset publicly available, these insights may be identified by any research team interested in these questions. The dataset is available in multiple formats with examples and additional technical details through the optical turbulence benchmark repository.

Funding. Office of Naval Research.

Acknowledgment. The authors would like to thank the Waterfront Readiness Center and the United States Naval Academy Mechanical Engineering, Electrical Engineering, Oceanography, and Mathematics Departments for their assistance in conducting the measurement campaign. We also thank the NOAA Coastal Observation program and the National Data Buoy Center for making data collected by their instruments available. The authors additionally thank the United States Naval Academy Trident Scholar for their early and continued support of this research effort.

Disclosures. The authors declare no conflicts of interest.

Data availability. The data underlying this study are publicly available as `usna_cn2_full` through [17], the optical turbulence benchmark repository [11].

REFERENCES

1. C. Jellen, J. Burkhardt, C. Brownell, *et al.*, "Machine learning informed predictor importance measures of environmental parameters in maritime optical turbulence," Appl. Opt, **59**, 6379–6389 (2020).
2. C. Jellen, C. Nelson, C. Brownell, *et al.*, "Measurement and analysis of atmospheric optical turbulence in a near-maritime environment," IOP SciNotes **1**, 024006 (2020).
3. L. C. Andrews and R. L. Phillips, *Laser Beam Propagation through Random Media* (SPIE, 2005).
4. R. Mahon, C. I. Moore, M. S. Ferraro, *et al.*, "Comparison of maritime measurements of C_n^2 with NAVSLaM model predictions," Appl. Opt. **59**, 10599–10612 (2020).
5. H. Wang, B. Li, X. Wu, *et al.*, "Prediction model of atmospheric refractive index structure parameter in coastal area," J. Mod. Opt. **62**, 1336–1346 (2015).
6. P. A. Frederickson, K. L. Davidson, C. R. Zeisse, *et al.*, "Estimating the refractive index structure parameter (C_n^2) over the ocean using bulk methods," J. Appl. Meteorol. **39**, 1770–1783 (2000).
7. C. Jellen, M. Oakley, C. Nelson, *et al.*, "Machine-learning informed macro-meteorological models for the near-maritime environment," Appl. Opt. **60**, 2938–2951 (2021).
8. "Scintec boundary layer scintillometer installation and operation manual" (2017).
9. M. Pierzyna, R. Saathof, and S. Basu, "π-ML: a dimensional analysis-based machine learning parameterization of optical turbulence in the atmospheric surface layer," arXiv, arXiv:2304.12177 (2023).
10. C. Jellen, C. Nelson, J. Burkhardt, *et al.*, "Hybrid optical turbulence models using machine-learning and local measurements," Appl. Opt. **62**, 4880–4890 (2023).
11. C. Jellen, C. Nelson, J. Burkhardt, *et al.*, "Effective benchmarks for optical turbulence modeling," arXiv, arXiv:2401.03573 (2024).
12. "Annapolis, MD - Station ID: 8575512," 2023, https://tidesandcurrents.noaa.gov/stationhome.html?id=8575512.
13. "User manual console for vantage Pro2 and vantage Pro2 plus weather stations" (2014).
14. "Station TPLM2 - Thomas Point, MD," 2023, https://www.ndbc.noaa.gov/station_page.php?station=tplm2.
15. D. Hassell, J. Gregory, J. Blower, *et al.*, "A data model of the climate and forecast metadata conventions (CF-1.6) with a software implementation (cf-python v2.1)," Geosci. Model Dev. **10**, 4619–4646 (2017).
16. D. Sadot and N. S. Kopeika, "Forecasting optical turbulence strength on the basis of macroscale meteorology and aerosols: models and validation," Opt. Eng. **31**, 200–212 (1992).
17. C. Jellen, C. Nelson, J. Burkhardt, *et al.*, "otbench: effective benchmarks for optical turbulence modeling," GitHub (2023), https://github.com/cdjellen/otbench.